Eur. Phys. J. C (2005)
Digital Object Identifier (DOI) 10.1140/epjc/s2005-02209-x

THE EUROPEAN PHYSICAL JOURNAL C

Low mass dimuon production in Indium-Indium collisions at 158 A GeV

The NA60 Collaboration

G. Usai[1,a], R. Arnaldi[9], R. Averbeck[11], K. Banicz[2,4], J. Castor[3], B. Chaurand[7], C. Cicalo[1], A. Colla[9], P. Cortese[9], S. Damjanovic[4], A. David[2,5], A. de Falco[1], A. Devaux[3], A. Drees[11], L. Ducroux[6], H. En'yo[8], A. Ferretti[9], M. Floris[1], P. Force[3], N. Guettet[2,3], A. Guichard[6], H. Gulkanian[10], J. Heuser[8], M. Keil[2,4], L. Kluberg[2,7], J. Lozano[5], C. Lourenço[2], F. Manso[3], A. Masoni[1], P. Martins[2,5], A. Neves[5], H. Ohnishi[8], C. Oppedisano[9], P. Parracho[2], P. Pillot[6], G. Puddu[1], E. Radermacher[2], P. Ramalhete[2,5], P. Rosinsky[2], E. Scomparin[9], J. Seixas[2,5], S. Serci[1], R. Shahoyan[2,5], P. Sonderegger[5], H.J. Specht[4], R. Tieulent[6], R. Veenhof[2,5], H.K. Wöhri[2,5]

[1] Università di Cagliari and INFN, Cagliari, Italy
[2] CERN, Geneva, Switzerland
[3] LPC, Université Blaise Pascal and CNRS-IN2P3, Clermont-Ferrand, France
[4] Universität Heidelberg, Heidelberg, Germany
[5] IST-CFTP, Lisbon, Portugal
[6] IPN-Lyon, Université Claude Bernard Lyon-I and CNRS-IN2P3, Lyon, France
[7] LLR, Ecole Polytechnique and CNRS-IN2P3, Palaiseau, France
[8] RIKEN, Wako, Saitama, Japan
[9] Università di Torino and INFN, Italy
[10] YerPhI, Yerevan, Armenia
[11] SUNY Stony Brook, New York, USA

Received: 22 February 2005 / Revised version: 8 March 2005 /
Published online: 8 July 2005 –

Abstract. The NA60 experiment studies open charm and prompt dimuon production in proton-nucleus and nucleus-nucleus collisions at the CERN SPS. During 2003 the experiment collected data in Indium-Indium collisions at 158 GeV per nucleon. Almost 240 million dimuon events were recorded. New results on J/ψ suppression, open-charm production and low mass dimuons should help clarify some interesting questions left open by previous experiments. After a brief detector description, this paper focuses on the analysis of the low mass dimuons. Preliminary results are presented on the ϕ/ω production cross section ratios and on the ϕ transverse momentum distributions, both as a function of collision centrality.

PACS. 25.75.Dw 25.75.Nq

1 Introduction

In the last 20 years, a considerable theoretical and experimental effort has been devoted to the search of the phase transition from nuclear matter to a deconfined state, the quark-gluon plasma (QGP). At the CERN SPS the heavy-ion program started in 1986 and for 15 years several experiments collected data. While many exciting results were found, several important questions remained unanswered.

The NA60 experiment is a second generation experiment which aims at clarifying some of those questions. Profiting from recent advances in silicon tracking detectors, new high precision measurements, impossible even just a few years ago, are now within reach. The NA60 physics program ranges from J/ψ suppression [1] and open charm production [2] to the investigation of the low mass dimuon region in proton-nucleus [3] and nucleus-nucleus collisions. In this paper we will focus on the study of this last topic.

The CERES experiment observed, in S-Au and Pb-Au collisions, an excess of electron pairs in the mass range 0.2–0.6 GeV/c^2, which cannot be explained in terms of expected sources (decays of light neutral mesons). This excess is located at low p_{T} and scales faster than linearly as a function of particle multiplicity [4]. These observations could be due to changes in the spectral function of the ρ meson, as expected in case the hot and dense medium produced in these collisions approaches a state where chiral symmetry is restored [5]. CERES is a truly pioneering experiment and made very interesting observations in extremely demanding experimental conditions. However, the measurements are hampered by lack of statistics, a rela-

[a] e-mail: gianluca.usai@ca.infn.it

tively modest mass resolution, and a challenging signal to background ratio. A clear interpretation of these results is still missing and will certainly benefit from a completely independent measurement, provided by a different experiment, using different tools and methods.

NA60 studied dilepton production in In-In collisions at 158 GeV per nucleon, by measuring dimuons rather than dielectrons. The very selective dimuon trigger and the use of fast detectors allowed us to take data at very high collision rates, leading to the collection of vast statistics. Moreover, the new silicon tracking detectors in the NA60 vertex region significantly improve the dimuon mass resolution, and the presence of a 2.5 T dipole field in the target region leads to a significant increase in the detection acceptance of low mass dimuons of low transverse momentum with respect to all previous dimuon experiments.

In this paper, we present first results on the ratio of the ϕ and ω production cross sections and on the ϕ transverse momentum distribution, both as a function of centrality. A more detailed understanding of the whole mass spectrum, including the continuum underlying the resonances, still requires further work.

2 Apparatus, detector concept and data taking

The NA60 apparatus is based on the 17 m long muon spectrometer previously used in the NA38 and NA50 experiments [6], separated from the target region by a 5.5 m long (mostly carbon) hadron absorber, and composed of eight multi-wire proportional chambers and four scintillator trigger hodoscopes, divided in "forward" and "backward" telescopes by the 5 m long ACM toroidal magnet. A 120 cm thick iron wall is located just before the last trigger hodoscope, and after the tracking chambers, to ensure that only muons can trigger the apparatus while not contributing to degrade the tracking accuracy.

The identification of muons provided by the "muon filter" leads to a very selective trigger, which allows the experiment to run at very high luminosities. On the other hand, the material which stops the hadrons also induces multiple scattering and energy loss on the muons, degrading the resolution of the measurement made in the spectrometer, especially in what concerns the angles of their trajectories.

NA60 overcomes this problem by complementing the muon spectrometer with silicon tracking detectors placed upstream of the absorber and close to the interaction vertex. The muon track can then be extrapolated to the target region and matched to one of the tracks measured by the silicon vertex telescope, significantly improving the final dimuon mass resolution. To cope with the high multiplicity and high interaction rate environment imposed by the study of rare processes in heavy-ion collisions, we must use high granularity detectors tolerant to record-breaking radiation levels. The silicon pixel detectors developed in the last few years, essentially aimed at the future LHC experiments, provide the technology break-through on which the NA60 detector concept is based. Without these innovative detectors, NA60 would certainly not exist.

The matching of the muon tracks before and after the hadron absorber also improves the signal to noise ratio, because many pion and kaon decays do not satisfy the matching criteria. Furthermore, the accurate reconstruction of the interaction vertices allows us to tag the two muon tracks according to their offset with respect to the interaction point, and with respect to each other at the position of the collision vertex. This allows us to tag and distinguish two dimuon event samples, "prompt" and "displaced" [2].

The Indium data sample was collected in 2003 with a silicon pixel telescope [7] made of 4-chip ("small") and 8-chip ("large") tracking planes. The basic detector elements ("chips" or "assemblies") are made of a silicon sensor, designed as a matrix of 256×32 pixels of 50×425 μm^2 area, each of them directly coupled (bump-bonded) to the corresponding cell of a readout pixel chip. The assemblies are glued to a multilayer hybrid circuit built on Al_2O_3 or BeO substrates. The ceramic support itself is glued and wire-bonded on a printed circuit board which provides mechanical support and routes the communication with the data acquisition system. Each plane has an average thickness of around 2 % X_0, mainly due to the sensor (300 μm), the readout chip (750 μm) and the gold used in the power and ground planes of the hybrid. The full tracking telescope provides 12 tracking points, thanks to eight small planes followed by four large "stations", each composed of two physical planes to cover the angular acceptance ($3 < \eta < 4$ or $35 < \theta < 120$ mrad) at larger distances from the target. The telescope is $\sim$26 cm in length starting at $\sim$7 cm downstream of the centre of the target system.

A schematic layout of the vertex region is shown in Fig. 1. In addition to the pixel telescope, a "beam tracker" made of four silicon microstrip detectors, arranged in two double stations and operated at 130 K, tracks the incoming ions such that we can deduce their transverse coordinates at the target with $\sim$20 μm resolution. While the vertex telescope determines the interaction point with an accuracy which improves from peripheral to central collisions, the measurement provided by the beam tracker is independent of the centrality of the collision, and allows us to control the systematic effects of the vertexing method. To measure the momentum of the charged particles, the vertex telescope is placed in a 2.5 T dipole field. Knowing the momentum is crucial to select the track which best matches the muon track, especially in the highest multiplicity collisions, where the knowledge of the angles is not sufficient.

The noise of the pixel detectors is only of the order of a few hundred electrons. Since the average charge produced by a passing particle is around 25 000 electrons, we can set threshold values which effectively eliminate the noise while keeping very high hit detection efficiencies and small cluster sizes. The innermost detector regions, closest to the beam axis, absorbed a total radiation dose equivalent to a flux of $\sim 10^{13}$ 1 MeV neutrons per cm^2. The continuous online monitoring of the detectors allowed us to follow the

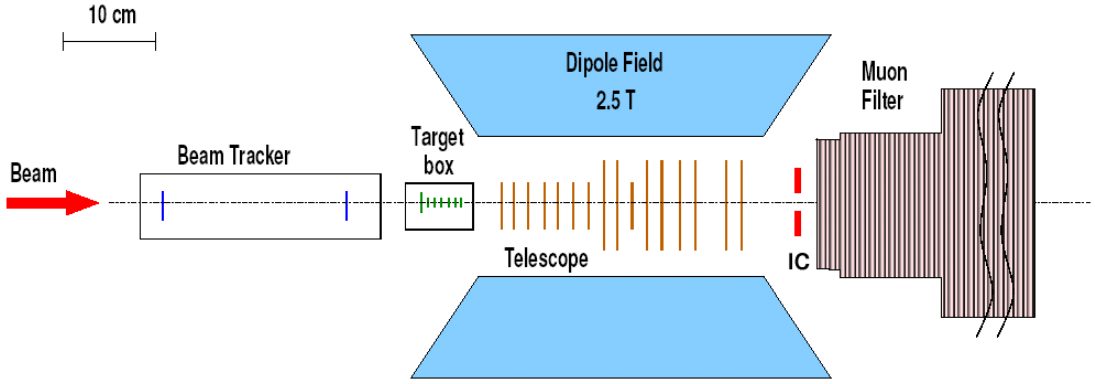

Fig. 1. Layout of the NA60 detectors in the vertex region

effects of the integrated radiation and, whenever needed, the bias voltages were increased. The detectors remained fully operational during the Indium run and several planes could still be used in the proton run of 2004, when they accumulated a similar radiation dose; the longer running period and the much higher collision rate compensated for the smaller track multiplicities per collision.

The data selected for final analysis corresponds to approximately 4×10^{12} ions incident on the targets. The average beam intensity was 5×10^7 ions per 4.8 s long spill, every 16.8 s. Seven 1.5 mm thick Indium targets were installed in a vacuum box, between the cryostat of the beam tracker and the vertex telescope. The transverse coordinates of the interaction point are determined with an accuracy better than 20 μm, while the z coordinate has a precision of around 200 μm.

3 Data reconstruction

The data reconstruction proceeds in several successive steps. First, the muon spectrometer tracks are reconstructed and events collected due to accidental triggers are rejected. Then we perform the pattern recognition and tracking in the pixel telescope, by far the most time consuming part of the reconstruction procedure. The muon spectrometer tracks are then extrapolated to the vertex region, taking into account multiple scattering and energy loss effects, and are matched to the tracks reconstructed in the pixel telescope. The matching is performed in terms of angles and momentum, comparing the slopes and curvature of the track in the vertex telescope with those of the muon extrapolated to the target. Every matching candidate is globally fit, using a Kalman filter, to merge together the information from the vertex telescope (better accuracy on the angles) and from the muon spectrometer (better momentum measurement). If both muons have at least one match, a joint fit is performed requiring that both muons converge to the same vertex. After selecting matched muon pairs, the combinatorial background of uncorrelated muon pairs from pion and kaon decays is still present, but to a lesser degree than in the original sample. This background is evaluated through a mixed event technique, combining single muons from different like-sign muon pairs, and only keeping pairs satisfying the trigger conditions. The measured like-sign muon pairs are used to normalize the mixed background and to verify the obtained shapes.

Central In-In collisions can result in up to 400 charged particles in the muon spectrometer's angular acceptance. Therefore, a muon track might be wrongly matched to a non-muon track in the pixel telescope. These "fake" matches must be carefully evaluated and subtracted, a non-trivial operation still on-going. The fraction of fake matches depends on the track multiplicity (collision centrality) and on the momentum of the muons (hence, on the dimuon mass). At the J/ψ mass the probability to have a wrong match is only a few percent, but at low dimuon masses it can reach almost 50 %. While waiting for the final algorithm to subtract fake matches over the full mass spectrum, Monte Carlo studies have been specifically performed to estimate the importance of this background in the study of low mass dimuons. It turns out that the study of the ϕ and ω production is barely influenced by the presence of fake matches, since these resonances stand out as well resolved peaks, thanks to the good mass resolution. However, a proper study of the underlying continuum, to search for thermal virtual photons and for changes on the (broad) spectral function of the ρ, will have to wait for the fakes subtraction.

4 Data analysis

Figure 2 shows the measured dimuon signal, after combinatorial background subtraction, integrating all collision centralities. It contains 370 000 events, with an overall signal to background ratio of 1/4, and corresponds to 35 % of the total collected statistics. The ϕ and ω peaks are clearly visible, each peak containing almost 40 000 events. The mass resolution is 23 MeV at the ϕ and does not depend on centrality. Also the η two-body decay peak is visible, for the first time in nuclear collisions.

The dimuon acceptance at low mass and low $p_{\rm T}$ has been significantly increased with respect to previous experiments. This major improvement is essentially due to the presence of the dipole field in the target region, which deflects to the angular acceptance of the muon spectrom-

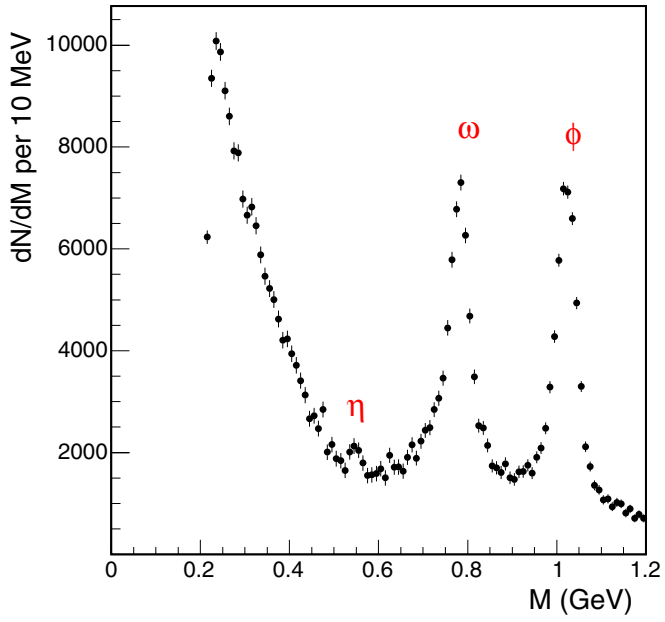

Fig. 2. Dimuon mass distribution after combinatorial background subtraction

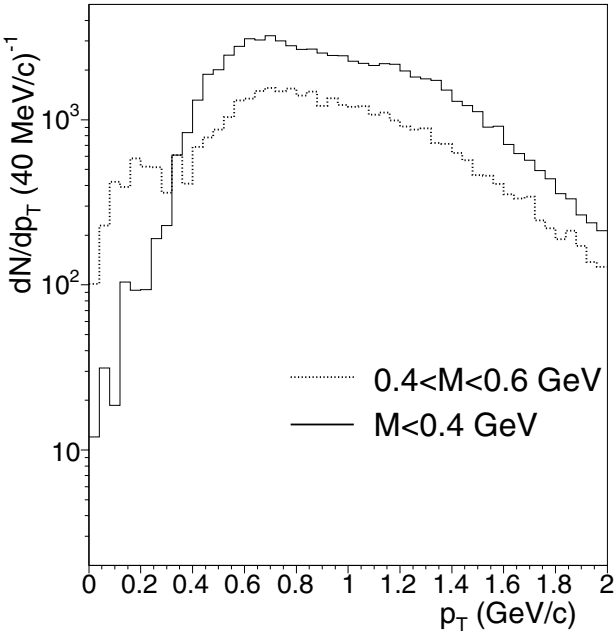

Fig. 3. $p_{\rm T}$ distributions of dimuons measured in semi-peripheral collisions, in two dimuon mass bins: 0.2–0.4 and 0.4–0.6 GeV/c^2

eter the low $p_{\rm T}$ opposite-sign muon pairs which would otherwise be lost in the dead area surrounding the beam line. The phase space coverage of our data is illustrated in Fig. 3, which shows the $p_{\rm T}$ distribution of the dimuons measured in the semi-peripheral multiplicity bin (second bin in Table 1), for two dimuon mass ranges.

For the analysis presented in this paper, the centrality of the Indium-Indium collisions was estimated from the measured multiplicity of charged particles. Four centrality bins have been defined, as shown in Table 1. For each bin, the corresponding value of the average number of participants, $\langle N_{\rm part}\rangle$, was evaluated from a Glauber fit to the forward energy spectrum, as measured in our zero-degree calorimeter (ZDC).

Table 1. Centrality classes

bins	$\mathrm{d}N_{\rm ch}/\mathrm{d}\eta$ range	$\langle \mathrm{d}N_{\rm ch}/\mathrm{d}\eta\rangle$	$\langle N_{\rm part}\rangle$
1	4–28	16	~ 20
2	28–92	70	91
3	92–160	145	161
4	>160	200	197

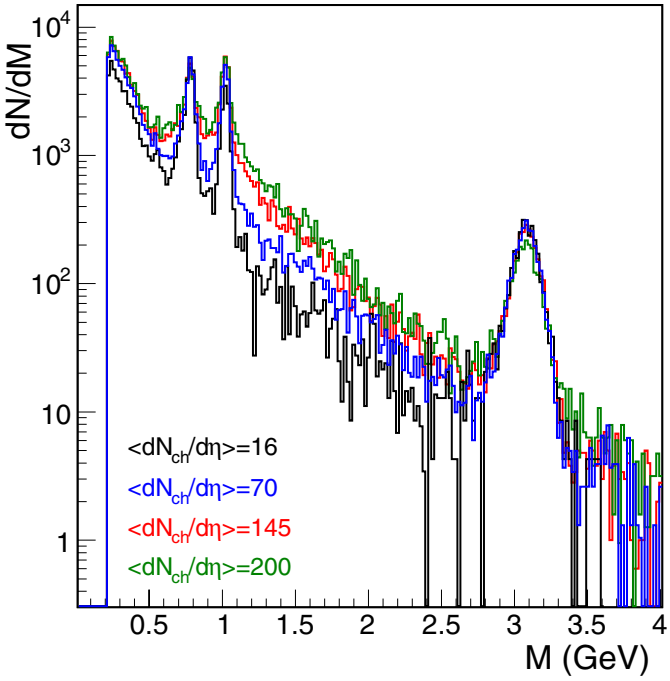

Fig. 4. Dimuon mass spectra for different collision centralities

Figure 4 shows the signal dimuon mass distributions, after combinatorial background subtraction, for the four centrality classes defined in Table 1. In order to more easily evaluate changes in the shape of the dimuon mass distribution between peripheral and central collisions, we have arbitrarily normalized the spectra with respect to each other at the ω peak. We see that, with the exception of the J/ψ region (and higher masses), the dimuon mass continuum both below and above the ω increases with charged particle multiplicity faster than the ω does. Although our Monte Carlo simulations indicate that the level of fake matches cannot account for this behaviour, we prefer to wait for the careful understanding, and subtraction, of the fake matches before extracting any conclusions from this observation. The situation is much cleaner in what concerns the ϕ peak which, like the ω peak, is very clearly defined in our mass distributions. Therefore, we can easily study the relative production cross-sections

of these two mesons, as well as the ϕ transverse momentum distributions. Preliminary results on these topics are presented in the next sections.

5 The ϕ/ω cross section ratio

In order to study the ϕ/ω cross section ratio, we must properly correct for the detection acceptances and efficiencies, which we have calculated through a detailed Monte Carlo simulation. We generated all the pertinent light meson decays, both dimuon and Dalitz, using the GENESIS code (see [3] for further details). A continuum source with an exponential fall-off beyond the ϕ was also included. The simulated events were then reconstructed in the same way as the real data. The contribution from fake matches to the continuum under the ω and ϕ peaks was realistically estimated by superimposing the simulated dimuons on tracks from real data.

We have then fitted the measured dimuon spectra, for each centrality bin, to a superposition of the simulated sources, leaving as free parameters the ratios η/ω and ϕ/ω, besides the continuum normalization. In this analysis we have assumed that the ρ and ω production cross sections are identical. The resulting ϕ/ω ratio is shown in Fig. 5 as a function of the number of participants. The same figure includes data points obtained by the NA50 experiment in Pb-Pb collisions at the same energy, 158 GeV per nucleon [8]. Before being included in this figure, the values published by NA50 were converted from the ratio $\phi/(\rho+\omega)$ to the ratio ϕ/ω, assuming $\sigma_\rho = \sigma_\omega$. Also the dimuon decay branching ratios were corrected for. In order to have both data sets reported in the same phase space region, we converted the NA50 points from the window $m_{\rm T} > 1.5$ GeV to the window $p_{\rm T} > 1.1$ GeV/c, assuming the inverse slope parameter $T = 228$ MeV, measured by NA50, for the extrapolation. The results obtained in this way for the two different collision systems (Pb-Pb and In-In) are in rather good agreement, suggesting that $N_{\rm part}$ is a good scaling variable to describe the ϕ/ω ratio. However, this conclusion should be seen as very preliminary until all the systematic uncertainties involved in the comparison are well understood.

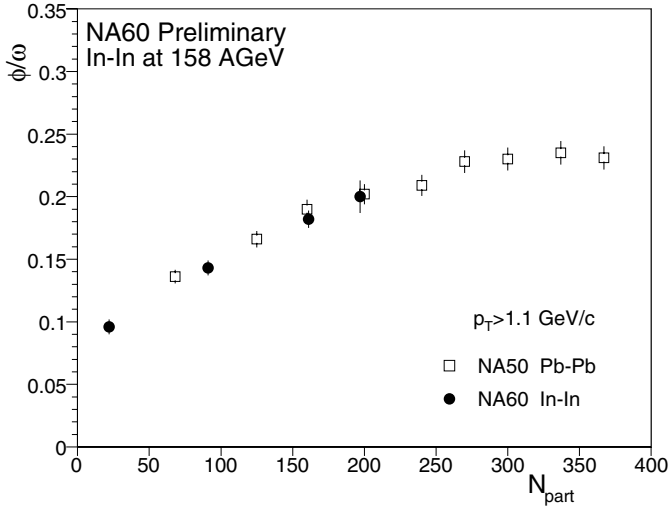

Fig. 5. The ϕ/ω production cross section ratio as a function of the number of participants

6 The ϕ transverse momentum

The ϕ transverse momentum distributions were studied by selecting signal dimuons in a narrow window around the ϕ mass. The background under the ϕ peak was evaluated and subtracted using two side windows symmetrically located around the peak. The probability that the detector accepts a ϕ meson with a certain $p_{\rm T}$ value depends on the corresponding dimuon rapidity. Therefore, we calculated the ϕ acceptance and pixel efficiency maps in y versus $p_{\rm T}$ cells, and made a 2-dimensional correction of the measured data. As before, the analysis was done for each centrality bin. The corrected 2-dimensional distributions were then projected on the $p_{\rm T}$ axis and fitted to the expression $1/p_{\rm T}\ {\rm d}N/{\rm d}p_{\rm T} \sim \exp(-m_{\rm T}/T)$, in order to determine the inverse slope parameter, T.

Figure 6 shows the measured transverse momentum distributions together with the fitted curves, for the 4 centrality bins. Once the full statistics will be analized, the $p_{\rm T}$ distributions should extend up to $\sim$3.5 GeV/c. There is a clear increase of the inverse slope parameter between peripheral and central Indium-Indium collisions, from $\sim$218 MeV to $\sim$255 MeV. Integrating over all collision centralities, we obtain $T = 252 \pm 3$ MeV. We do not see any dependence of T on the rapidity of the ϕ meson. In order to check the stability of the results, we have changed the position and width of the side bins used to subtract

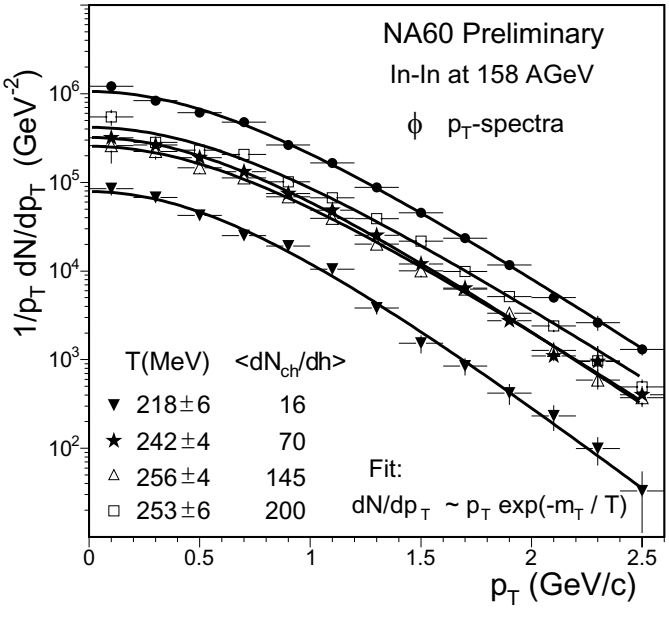

Fig. 6. The ϕ transverse momentum distributions for four different collision centrality bins, as labeled on the figure, and for the sample integrated over centrality (closed circles)

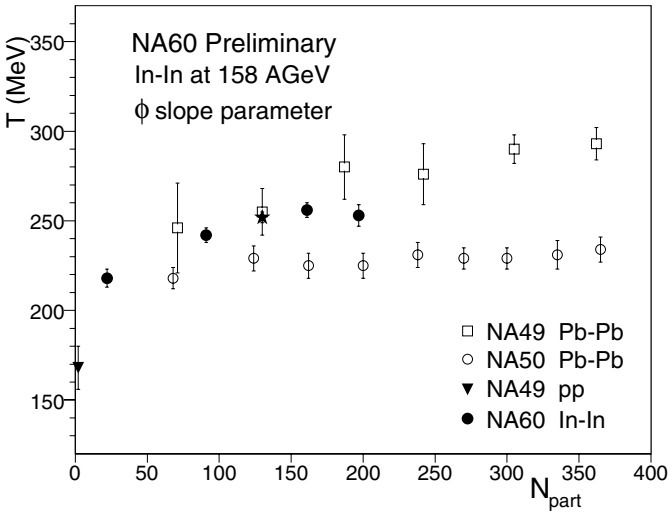

Fig. 7. The ϕ inverse slope parameter, T, as a function of the number of participants

the background. The results are quite insensitive to such changes. Also the acceptance correction plays a minor role since, at the ϕ mass, it does not change by more than a factor of 2 over the full $p_{\rm T}$ range.

Figure 7 shows how the T values extracted from our data vary with the number of participants, in comparison with measurements previously done in Pb-Pb collisions by the NA49 [9] and NA50 [8] experiments, using $\phi \to KK$ and $\phi \to \mu\mu$ decays, respectively. Our analysis was repeated restricting the data to $p_{\rm T} < 1.5$ GeV/c (corresponding to the NA49 range) and to $m_{\rm T} > 1.5$ GeV (corresponding to the NA50 range), with almost identical results. The significant increase of T with $N_{\rm part}$ seen in our data, and also in the data of NA49 (with bigger uncertainties), seems to be in contradiction with the observations of NA50, which report "temperatures" independent of the collision centrality. To further clarify this issue, a completely independent analysis is currently in progress, to study the ϕ properties through the $\phi \to KK$ decay, thanks to the good quality of the data collected by the silicon vertex telescope.

7 The ϕ mass as a function of centrality

We have also started a study aimed at seeing if the ϕ mass changes as a function of the collision centrality. At the present moment, the estimated precision achievable in this measurement is around 3 MeV, within which no change has been observed. Changes in the width of the ϕ are much harder to detect, with a 23 MeV mass resolution. The $\phi \to KK$ study should improve our sensitivity in this respect, since the mass resolution for this final state is expected to be around 8 MeV .

Summary

The NA60 experiment collected a high-statistics sample of dimuon events, produced in high-energy Indium-Indium collisions, with rather good mass resolution and signal to background ratio. In the present paper we have concentrated on the study of the low mass vector mesons, ω and ϕ. Preliminary results have been given in what concerns their cross-section ratio and the $p_{\rm T}$ distribution of the ϕ, in both cases as a function of the collision centrality. The analyzed event sample is around one third of the statistics on tape. Presently, our efforts are concentrated on the determination and subtraction of the fake matches component, so that we can also address the physics of the low mass dilepton continuum, where the CERES collaboration has made very interesting observations, both in S-Au and in Pb-Au collisions, by measuring electron pairs. Our low mass dimuon measurements will surely lead to an important progress in the understanding of low mass dilepton production, and its relations with the physics of the dense and hot QCD matter created in high-energy nuclear collisions.

Acknowledgements. Several people contributed to the feasibility of the measurements reported in this paper, including M. Burns, M. Campbell, L. Casagrande, B. Cheynis, E. David, J. Fargeix, W. Flegel, L. Gatignon, V. Granata, J.Y. Grossiord, F. Hahn, S. Haider, E. Heijne, A. Kluge, L. Kottelat, D. Marras, I. McGill, T. Niinikoski, R. Oliveira, A. Onnela, V. Palmieri, P. Riedler, J.M. Rieubland, J. Rochez, M. Sanchez, W. Snoeys, G. Stefanini, H. Vardanyan and K. Wylie. Zheng Li developed and produced the silicon sensors of the Beam Tracker at BNL and Kurt Borer built the corresponding read-out electronics chain at LHEP, Bern.

References

1. R. Arnaldi et al. (NA60 Coll.), Eur. Phys. J. C **43** (2005)
2. R. Shahoyan et al. (NA60 Coll.), Eur. Phys. J. C **43** (2005)
3. H.K. Wöhri et al. (NA60 Coll.), Eur. Phys. J. C **43** (2005)
4. G. Agakichiev et al. (CERES Coll.), Phys. Rev. Lett. **75**, 1272 (1995); Phys. Lett. B **422**, 405 (1998); B. Lenkeit et al. (CERES Coll.) Nucl. Phys. A **661**, 23c (1999)
5. R. Rapp, J. Wambach, Adv. Nucl. Phys. **25**, 1 (2000); G.E. Brown, M. Rho, Phys. Rep. **363**, 85 (2002)
6. C. Lourenço, PhD thesis, IST, Lisbon, Portugal, 1995
7. M. Keil et al., Nucl. Instrum. Meth. A **539**, 137 (2005)
8. D. Jouan et al, (NA50 Coll.), J. Phys. G **30**, S277 (2004); B. Alessandro et al. (NA50 Coll.), Phys. Lett. B **555**, 147 (2003)
9. V. Friese et al. (NA49 Coll.), Nucl. Phys. A **698**, 487c (2002)